AFRL-RV-HA-TR-2008-1006

Anomalous Conditions in the Middle Atmosphere During Boreal Winters of 2004 and 2006

Peter P. Wintersteiner

ARCON Corporation
260 Bear Hill Road
Waltham, MA 02451-1080

Scientific Report No. 3

31 December 2007

AIR FORCE RESEARCH LABORATORY
Space Vehicles Directorate
29 Randolph Road
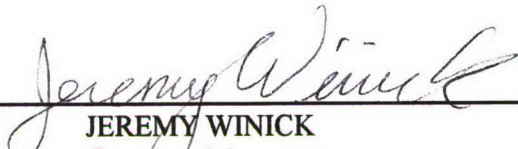**AIR FORCE MATERIEL COMMAND**
Hanscom AFB, MA 01731-3010

20080311227

NOTICE AND SIGNATURE PAGE

Using Government drawings, specifications, or other data included in this document for any purpose other than Government procurement does not in any way obligate the U.S. Government. The fact that the Government formulated or supplied the drawings, specifications, or other data does not license the holder or any other person or corporation; or convey any rights or permission to manufacture, use, or sell any patented invention that may relate to them.

This report was cleared for public release and is available to the general public, including foreign nationals. Qualified requestors may obtain additional copies from the Defense Technical Information Center (DTIC) (http://www.dtic.mil). All others should apply to the National Technical Information Service.

AFRL-RV-HA-TR-2008-1006 HAS BEEN REVIEWED AND IS APPROVED FOR PUBLICATION IN ACCORDANCE WITH ASSIGNED DISTRIBUTION STATEMENT.

JEREMY WINICK
Contract Manager

PAUL TRACY, Acting Chief
Battlespace Surveillance Innovation Center

This report is published in the interest of scientific and technical information exchange, and its publication does not constitute the Government's approval or disapproval of its ideas or findings.

REPORT DOCUMENTATION PAGE

Form Approved
OMB No. 0704-0188

1. REPORT DATE (DD-MM-YYYY)	2. REPORT TYPE	3. DATES COVERED (From - To)
31/12/2007	Scientific Report No. 3	8-01-2006 to 7-31-2007

4. TITLE AND SUBTITLE
Anomalous Conditions in the Middle Atmosphere During Boreal Winters of 2004

5a. CONTRACT NUMBER
FA8718-04-C-0031

5b. GRANT NUMBER

5c. PROGRAM ELEMENT NUMBER
61102F

6. AUTHOR(S)
Peter P. Wintersteiner

5d. PROJECT NUMBER
2301

5e. TASK NUMBER
SB

5f. WORK UNIT NUMBER
A1

7. PERFORMING ORGANIZATION NAME(S) AND ADDRESS(ES)
ARCON Corporation
260 Bear Hill Road
Waltham, MA 02451-1080

8. PERFORMING ORGANIZATION REPORT NUMBER

9. SPONSORING / MONITORING AGENCY NAME(S) AND ADDRESS(ES)
Air Force Research Laboratory
29 Randolph Road
Hascom AFB, MA 01731-3010

10. SPONSOR/MONITOR'S ACRONYM(S)
AFRL/RVBYM

11. SPONSOR/MONITOR'S REPORT NUMBER(S)
AFRL-RV-HA-TR-2008-1006

12. DISTRIBUTION / AVAILABILITY STATEMENT
Approved for public release; distribution unlimited.

13. SUPPLEMENTARY NOTES

14. ABSTRACT

An examination of SABER data for boreal winter reveals extraordinary conditions in the mesosphere early in 2004 and 2006. In portions of the polar region, during much but not all of the mid-January through mid-March period for which data are available in each of those years, the OH layer is unusually low and bright. The temperature structure in also greatly perturbed, from the stratosphere to the upper mesosphere. Specifically, the OH layer is found as much as 8 km below its nominal altitude of 87 km, and very high temperatures – occasionally exceeding 275 K – appear at altitudes where the layer exists. We use SABER data to quantify the anomalous effects, study their evolution, and contrast them with those of the "normal" years 2003 and 2005. We also cite other observations and model studies of conditions in the stratosphere during those years, and enhanced downward transport within the polar vortex that has been inferred from them. Transport is the likely explanation for the anomalous properties of the OH layer seen in the SABER data.

15. SUBJECT TERMS
Hydroxyl, OH layer properties, Mesosphere, Volume emission rate, Limb radiance, Temperature retrieval, Polar vortex, NOx, Boreal winters 2004 and 2006, Temperature inversion layer

16. SECURITY CLASSIFICATION OF:			17. LIMITATION OF ABSTRACT	18. NUMBER OF PAGES	19a. NAME OF RESPONSIBLE PERSON
a. REPORT	**b. ABSTRACT**	**c. THIS PAGE**	SAR	38	Jeremy Winick
U	U	U			19b. TELEPHONE NUMBER (include area code)

Standard Form 298 (Rev. 8-98)
Prescribed by ANSI Std. 239.18

Table of Contents

List of Figures

1. INTRODUCTION

This Interim Scientific Report describes work that was undertaken according to the provisions of contract #FA8718-04-C-0031. Most of this work was done during the third year in which it was in effect, that period being 1 August 2006 through 31 July 2007.

The purpose of this report is to document very unusual conditions that were observed in the stratosphere and mesosphere in northern-hemisphere winters of 2004 and 2006, and to contrast them with what was seen during "normal" years. The anomalous conditions occurred at high latitudes, mostly but not entirely in polar night. The observations are those of the SABER instrument on the TIMED satellite. The quantities to which we mainly direct our attention are those describing the OH layer in the upper mesosphere, but we also examine retrieved temperature in both the mesosphere and stratosphere.

This investigation originally sprang from work we were doing on double-peaked OH layers. Such layers were observed frequently in the airglow by the WINDII instrument aboard UARS [*Melo et al, 2000*] and are also common in SABER data. Having done much work on large temperature inversion layers (TILs) [*Winick et al., 2004; Wintersteiner and Cohen, 2005*], we sought to verify the suggestion that TILs could be responsible for OH double layers. We searched more than a year's worth of SABER events from the entire globe, separating data according to season, latitude, and local time (LT). We found that while there were strong variations in the appearance of both TILs and double layers within this parameter space, the correlation between them that we were seeking was lacking [*Winick et al., 2005*].

The latitude/LT/season variability in OH, however, is interesting in itself. Much of it, apparently driven by the tides, conforms with previous observations, but we also documented the existence of extremely low and bright OH layers in winter 2004 [*Winick et al., 2006*]. As there is no record in the literature of such unusual behavior, we became interested in making a systematic study of these conditions in an attempt to understand them. That is the motivation for the present work.

2. MIDDLE-ATMOSPHERE ANOMALIES IN 2004 AND 2006

2.1. Background

Conventionally, OH airglow emission is described as originating in a single layer that is approximately symmetric vertically, centered at about 87 km. It arises because of the chemical reaction,

$$H + O_3 \rightarrow OH(v) + O_2,$$

which produces excited vibrational states of OH that quickly lose some of their energy by emission in different vibrational bands. When observed by satellite instruments, the resulting limb radiance can be inverted to produce the volume emission rate (VER, with units of energy per unit volume per unit time). The inversion procedure is relatively straightforward, so long as the emission at a particular altitude does not vary in the horizontal direction, because the bands are all optically thin.

The OH data that we examine is from the SABER instrument on the TIMED satellite. The acronyms are <u>T</u>hermosphere <u>I</u>onosphere <u>M</u>esosphere <u>E</u>nergetics and <u>D</u>ynamics—

reflecting that the satellite's mission is to study the energy balance of the mesosphere and lower thermosphere (MLT) region—and Sounding of the Atmosphere by Broadband Emission Radiometry. SABER [*Russell et al., 1999*] is a ten-channel radiometer. Since early in 2002, it has been continuously scanning the limb between the ground and tangent heights of approximately 300 km, recording IR and NIR emissions from several emitters. Its nearly-continuous duty cycle, the high-inclination TIMED orbit, and sensitive detectors enabling high-altitude measurements, combine to produce near-global coverage for many data products.

Two of the channels, at 2.0 μm and 1.6 μm, are used for OH. Designated OH-A and OH-B, respectively, they respond to Δv=2 transitions: primarily 9-7 and 8-6 for OH-A, and 5-3 and 4-2 for OH-B. Volume emission rates are obtained from Abel inversions, taking into account the incomplete spectral coverage of the instrument by use of a so-called "unfilter factor" [*Mlynczak et a., 2005*]. The VERs are Level 2 data products, and most of what we used is from version 1.06.

Meanwhile, SABER CO_2 15 μm limb radiance is used to retrieve atmospheric temperature and pressure up to ~100 km, much higher than was previously possible. This is accomplished by a new non-LTE retrieval algorithm [*Mertens et al., 2001; 2002; 2004*]. All temperatures that we cite are from version 1.06.

The precession of the TIMED orbit is such that local times of the equator-crossings decrease by about 0.2 hours per day. It takes almost 60 days to view all accessible local times, between the ascending and descending portions of the orbit, so there is a correlation between LT and the acquisition date of the data. Times near local noon cannot be observed at all because of detector sensitivity. When the satellite precesses so the instruments point to within a certain angle close to the Sun, a yaw maneuver is performed and a new ~60-day "yaw cycle" is begun. There are six cycles every year, beginning and ending on nearly the same dates each year. Three of them are so-called "north-viewing" cycles, the latitude range at the tangent point being between ~83°N and ~51°S on each orbit. The "south-viewing" yaw cycles have the opposite range, ~83°S to ~51°N.

The north-viewing yaw cycle of most interest for present purposes begins on January 15 and lasts through March 18 each year, give or take a day. Since SABER cannot view the winter north-polar region prior to January 15, the 2004 data that originally attracted our attention were entirely within this period; the earliest part of winter 2003-2004 was inaccessible. We later examined data from this yaw cycle in other years as well, and July-September cycles viewing south-pole winters.

2.2. Observations of the OH Layer

2.2.1. Analysis

Our systematic examination of OH layer characteristics began by constructing lists of all single-peak nighttime measurements from particular yaw cycles. "Nighttime" events, for our purposes, were all those for which the solar zenith angle (SZA) was greater than 105° at 80-km altitude. The lists contained—in addition to event-identifying parameters such as date, location, SZA, etc.—characteristics of the OH layer such as its brightness, altitude, and width. "Brightness" is defined as the maximum value of the VER profile, altitude is where that maximum occurs, and we use full width at half maximum. We also

calculated the temperature and pressure at the layer altitude. All these parameters were determined using VER data from OH-A and OH-B, separately.

Figure 1 shows three OH-B profiles from January 23, 2004. One profile is a very low, bright layer centered just below 78 km—typical of the anomalous conditions of present interest. (The very lowest individual layers we observed were at ~75 km.) Another is a "normal" layer at ~87 km, from a lower-latitude event. The third is a double peak, of the sort we eliminate before considering the aggregate properties of the region. The Appendix describes our algorithm for determining layer properties and removing double peaks.

There are alternative ways to determine layer properties, and we calculated several of them. The zenith radiance (VER integrated vertically) is an alternative measure of emission intensity. Brightness-weighted mean altitude is an alternative measure of layer height. Brightness-weighted temperature is a commonly-used quantity, since that is what is usually calculated using data from ground-based instruments which have no means of altitude discrimination. Brightness-weighted averages use VER as the weighting profile.

Considering that there are different ways of determining parameters, a certain ambiguity is inherent in any of them. This is particularly true of layer altitude. VER profiles are not actually symmetric, although they are often treated as if they were. Profiles are usually steeper on the lower side than on the upper (as with the two single-peak events in Figure 1). This is the result of different gradients (of opposite sign) in the densities of O_3 and H. Differences in quenching across the layer may also have some effect on the shape. The upshot is that layer altitude determined from the peak of the VER profile is ~1-2 km lower than that determined by brightness-weighting.

There are also differences between OH-A and OH-B. Comparing the two, it is noteworthy that the nascent reaction directly populates vibrational states $v=6\text{-}9$, while the lower states are populated largely because of quenching, due to collisions of higher ones. With slightly higher quenching rates in the lower portion of the layer, the $v=5$ and $v=4$ states responsible for the OH-B emissions are somewhat more highly populated there than in the upper portion of the layer. The OH-B layer altitude typically appears about 1.5 km lower than the OH-A altitude. The VERs of the two emissions are also different, OH-B being ~2-3 times brighter.

As noted above, we partitioned large numbers of SABER events according to latitude and local time. The point was to characterize the OH layer by calculating averages of altitude, brightness, etc. These averages are zonal-mean quantities, because the full range of longitudes is observed each day, while local time varies quite slowly.

We generally worked with 3- or 6-degree latitude bins, and we always used 1-hour local time bins. Except at the extreme northern and southern parts of the orbit (the "turn-around points"), a 3-degree/1-hour bin contains, typically, 12 to 16 events per day or approximately one event per orbit, discounting dropouts. At a precession rate of ~0.2 hours/day, events in most 1-hour LT bins accumulate in about 5 days. However, for bins near local midnight, there are events at the beginning and the end of each yaw cycle. As the respective acquisition dates are nearly two months apart, it is important to be aware that there are events in those LT bins from each period, and distinguish them if necessary.

The restriction to single-peak VER profiles eliminates approximately 20-25% of all SABER nighttime events. Of those removed, some have double peaks in only one of the two profiles. One reason for imposing this restriction is the inherent ambiguity in specifying peak altitude and width. Another is the possibility that some of the double peaks reflect laterally inhomogeneous conditions, rather than an actual disruption of the region due to some physical phenomena like TILs or gravity waves. This would violate a basic premise of the Abel inversion (and, indeed, it is hard to see how short-wave gravity waves would not do that in any case) and, thereby, call the retrieval into question [*Winick et al., 2005*]. We note that, if multiple-peak events were included, zenith radiance and/or brightness-weighted parameters could be more useful parameters than the ones we chose.

2.2.2. Seasonal Dependence

Figure 2 shows the mean OH layer altitude determined using OH-B for the four yaw cycles covering the period from mid-March through mid-November, 2004. The altitude range is ~85-88 km in all four periods. Latitude/LT dependence appears clearly in all of them, and it is practically the same in all but the May-July cycle. In the equatorial region, in those three periods, the layer is lower in the evening and rises in the post-midnight hours. At mid-latitudes, ~25-40°, it seems to have both a maximum and a minimum during the nighttime hours. In the May-July cycle, the pattern is different. The rms deviation of these measurements (not shown) is typically less than ~1.5 km, but there is a systematic increase to ~2.5 km in the postmidnight hours at the equator. (See later discussion, and Figure 4e.) The periods November 2004 to January 2005 (not shown) and January-March 2005 (in Figure 4c) are also similar in all these respects.

Figure 3 shows the peak VER from OH-B in the same format. As with altitude, there is a strong latitude/LT dependence that is very similar during three of the four cycles and in the two following ones that are not shown here. As before, the May-July period is different. One sees that the peak VER varies by a factor of two, and comparing Figures 2 and 3, it is clear that the brightest periods correlate with the lowest altitudes.

Layer altitude and brightness derived from OH-A show the same dependencies that are evident in these figures.

Considering that the diurnal and semidiurnal atmospheric tides have their maximum amplitudes at equatorial and mid-latitude regions, respectively, the LT-dependence shown in both of these figures can be attributed to tidal effects. That is, as nearly as one can tell, altitude and brightness have both a minimum and maximum at mid-latitudes within the nighttime hours, whereas, at the equator, the data suggest diurnal dependence (trends rather than oscillations). Of course, it is well known that tides and associated photochemistry affect OH emissions [e.g., *Zhang and Shepherd, 1999*]. We made a very brief comparison [*Winick et al., 2005*] of data from SABER with the WINDII data they cite. We found, comparing the same seasons in 2004 and 1992, respectively, that although the basic picture was similar, there were differences in the LT dependence.

2.2.3. OH in Polar Winter

Figure 4 compares four years of SABER data during the January-March north-looking yaw cycle. The 2004 altitudes in the polar region originally caught our attention because the OH-B zonal mean turned out to be lower than 80 km in some cases. This is far below

the nominal layer height of 87 km, and well out of range of the expected variability. An intercomparison of the altitude for winters 2003 through 2006 [Figures 4(a-d)] reveals that in 2003 (a) and 2005 (c), the layer height is "normal" (~86 km) in the polar region. In general, these plots look similar to those in Figures 2a, 2c, and 2d. It also shows that the polar region has unusually low layers not only in 2004 (b) but also in 2006 (d). Except for the northernmost region, however, the latter plots are similar to those for other years and most other seasons.

Figures 4e and 4f compare the rms deviations of the layer altitudes for two years, 2003 and 2004. In 2003, the variance is on the order of only ~1 km for most of the parameter space, except for a few bins near 60°N and all the post-midnight bins near the equator. (As noted above, the latter result appears for all seasons.) In 2004, in contrast, there is a much larger variance in the north polar region. Results for 2005 and 2006 (not shown) are much like those for 2003 and 2004, respectively.

Figure 5 shows the layer brightness for the four years. For the anomalous years 2004 and 2006, one sees much brighter emissions in polar winter in exactly the bins where the low layer altitudes are recorded. For the "normal" years, OH-B emissions are less than half as intense as in the corresponding anomalous bins during the unusual winters.

All the comparisons that we have made using OH-B could be made equally well with OH-A. The only difference, noted earlier, is that the OH-A layer is slightly higher. Also, although our analysis has not been as thorough as for 2003-2006, years 2002 and 2007 both appear to have "normal" OH layer characteristics in boreal winter.

An obvious question is whether the anomalous behavior of the OH emissions in 2004 and 2006 existed throughout the ~60-day yaw cycle. This is relevant because each latitude/LT plot uses data from the entire yaw cycle. The short answer is that, in both years, the low bright layers had disappeared by early March. In Section 2.4., we will address evidence for this and discuss how it affects our results.

2.3. Middle Atmosphere Temperature

2.3.1. Anomalies in 2004 and 2006

It turns out that, in boreal winters of 2004 and 2006, SABER-retrieved temperature also has very unusual characteristics. Figure 6 compares zonal-mean temperature in the latitude range 75-78°N on each of two days in 2004, 2005, and 2006. One can see that in 2005, the temperature structure on both days has a familiar appearance. The stratopause appears near 50 km. The mesopause is high, at ~95-100 km, with temperatures near 180 K on one day and 200 K on the other. The main difference in 2005 is the large TIL appearing on January 19, which is absent on February 4. In fact, at these latitudes, the occasional appearance of TILs accounts for the only significant variability in daily zonal-mean temperature, which is otherwise very consistent throughout the yaw cycle. This is true for latitudes down to at least 66°N.

Year 2004 (red in Figure 6) presents a stark contrast. Near the normal stratopause altitude, a clear temperature <u>minimum</u> exists on both days. A 260-K stratopause, if it can be called that, is found at altitudes of ~75 km. The temperature at the nominal OH layer height is considerably warmer than in 2005. Only the mesopause appears normal.

In 2006, the temperature is quite different on these two days. On January 19, it looks "normal," not dissimilar from 2005; a relatively cold stratopause near 45 km, a 195-K mesopause near 95 km, and little structure inbetween. The February 4 profile, however, is completely unconventional, with a maximum (~260 K) at 80 km and a nearly constant temperature of ~220 K from 25 to 60 km. On that day, conditions appear to be more like those in 2004 than in 2005.

There are also considerable differences in the variance for each of these six zonal-mean profiles. The small (~4-6 K) uniform spread that is seen over the full range on February 4, 2006, contrasts with much larger variance (~15 K) of several other profiles at some or all altitudes. For example, the January 19, 2004, profile has small variance from ~25-50 km and a much larger one near the 80-km "stratopause." In 2005, the spread is greater than ~10-12 K above 50 km. The implication of this is that there is distinct zonal asymmetry in temperature on many, but not all, of the days shown and, moreover, that it is altitude dependent. In 2004, the January 19 profile, especially, suggests zonal symmetry at low altitudes but considerable longitude-dependence above ~55 km.

To investigate the temperature variability in a more comprehensive fashion, we made maps of the northern hemisphere showing temperature in false color at several pressure levels at different times during the yaw cycles in each of three years, 2004-2006. A small subset of these appears in Figures 7 and 8, where stratospheric (top) and mesospheric (bottom) temperatures are plotted for January 18-19 and February 7-8, respectively, in each of the three years, 2004-2006. These figures are insufficient for documenting the evolution of middle-atmosphere temperature during these winters, but they do reveal structure and variability that can be related to the appearance of the profiles in Figure 6.

In the "normal" year of 2005, there is a warm upper stratosphere with a discernible wave-one pattern, much like that in Figure 7b, persisting from January through mid-March. This is more clearly evident at 0.5 hPa (not shown) than at 2 hPa and is consistent with the moderately large variance in Figure 6 for corresponding altitudes. The mesosphere, on the other hand, shows little zonal structure throughout the yaw cycle. Structure that does exist there tends to anticorrelate with that at 0.5 hPa—that is, somewhat cooler mesospheric temperatures where the stratosphere is warmer—but it is not remarkable.

In 2004, a very cold upper-stratospheric vortex exists throughout the yaw cycle until about March 6. This feature can be seen clearly in Figures 7a and 8a. Although it is persistent and strong, it tends to be variable in size, and seems to be centered at various locations—generally at western longitudes—that are ~10-15 degrees south of the pole. (Due to absence of data above ~83°N, it is difficult to be precise about this.) In 2006, a vortex exists throughout most of the month of February, e.g., Figure 8c, but is absent in January (Figure 7c) and March. There is no sign whatsoever of such a cold structure in the stratosphere in 2005.

Mesospheric temperatures in 2004 and 2006 are complementary to those in the stratosphere. Specifically, in the 0.005-0.002 hPa range (normally ~82-89 km), they are very high in the same locations where they are low in the stratosphere (Figures 7d, 8d, 8f). At the high-altitude end of this range, temperature regularly exceeds 240 K, and it is even warmer lower down, in accord with the 2004 plots and the February 4, 2006 plot in Figure 6.

2.3.2. Correlation with Unusual OH Layers

The coincident appearance of such unusual temperature structures and OH layer characteristics strongly suggests a connection between the two, if not necessarily a cause-and-effect relationship. Figure 9 shows maps of the OH layer altitude, and temperature at that altitude, for February 7-8, 2004. (This temperature plot should be distinguished from those in earlier figures, which give temperature at particular pressure levels.) The minimum in layer altitude in Figure 9a, offset from the pole, correlates very closely with the offset maximum in temperature in 9b, which exceeds 270 K in one segment of the polar region that reaches down to about 75°N. The extended region where temperature exceeds 240 K is very nearly the same as that for which the layer altitude is below 80 km.

Figure 10 contrasts the OH layer altitude on January 18-19, 2004, with that on the same dates in 2005. Comparison of Figure 10a with Figure 7d shows, as before, a high correlation between regions of unusual temperature and those of unusual layer height. Comparison of Figures 10a and 10b, on the other hand, shows that the asymmetry about the pole that is prevalent in 2004 is absent in 2005, when the layer appears in a uniformly narrow range of altitudes between ~84 and 86 km. There are other dates in 2005 (not shown) when the longitude-dependence is greater, but on most of those days, the broader range extends upwards, above 87 km, rather than downwards.

2.4. Variability

The anomalous temperatures and OH layers appearing in 2004 and 2006 are clearly distinct from climatological means, but there is considerable additional variability within the 60 days for which data is available in each of these winters. This includes varying zonal asymmetry in temperature, which we inferred from the variance of zonal-mean profiles (Figure 6), and which is also directly apparent in northern-hemisphere maps. It also includes the temporal evolution of the regions with anomalous temperature and OH.

To visualize these day-to-day changes, we defined certain measures of "anomalous" OH layer height and temperature, determined the approximate area of the polar region that could be so characterized, and then observed how this evolved during the winter.

We use 82 km as a threshold for OH-B layer heights and 230 K as a threshold for temperature. We assert that anomalous conditions exist in regions where mean layer heights fall below that altitude, or where the atmosphere is warmer than that temperature. In so doing, we refer to the altitude at which the OH-B VER profile maximizes and to the "layer temperature" at that altitude. We also did this with OH-A, using cutoffs of 83.5 km and 227 K. We divided the Earth's surface into moderately sized latitude/longitude bins and found the average layer height and layer temperature, using all single-peak nighttime events occurring within each bin during periods of a few days. The bin size was 6 degrees in latitude by 15 degrees in longitude, and we used 6-day periods. These choices assured that there would be enough events per bin to get a meaningful average; other combinations, however, produce similar results. Finally, we added up the total area of all the anomalous bins for each period and plotted the result, expressed as a percentage of the total surface area of Earth.

Figure 11 shows the results for the January-March period in 2004 and 2006, using low OH layers as the criterion for anomalous conditions. For 2004, one sees that at the begin-

ning of the yaw cycle, there is a large anomalous area, but it diminishes in size toward the end of January. By the second week of February, however, it had grown again, briefly covering ~4% of the Earth's total surface before decreasing and finally disappearing early in March. (For comparison, the entire area north of 60° is 6.7%.) In 2006, the anomalous region forms in late January, reaches its maximum in early February, and is gone by the first few days of March. In 2003 and 2005, no latitude/longitude bin qualifies as anomalous, by this standard, for any 6-day period during the winter yaw cycle. We note that the extreme northerly region is never observed by SABER and has, therefore, been excluded from the calculation. Since many of the polar maps suggest that most, or all, of this region would be classified as anomalous, the figure undoubtedly understates the actual area. The excluded area is 0.4% of the globe, but the point of this is the variation with time, not the absolute area in question.

These plots show that using the layer altitude from OH-A, instead of OH-B, produces almost exactly the same result for temporal changes.

Figure 12 shows anomalous characteristics in a similar fashion, using layer temperature rather than layer altitude as the criterion. For 2004, the evolution of the anomalous region proceeds as it did when defined by altitude. For 2006, the area evolves from late January on, in nearly the same fashion as in Figure 11b. The main difference between Figures 11b and 12b is the existence of a high-temperature region in mid-January, when there was no low-layer region. Our investigation revealed an isolated high-temperature region located near ~55°N, 270°E, at this time, having no apparent connection to the polar region or any correlation with low OH layers. Note, the southern extreme of the anomalous regions found on any of our maps of OH layer altitude is at about this latitude.

Figure 13 shows zonal-mean temperature profiles once again, this time for three days near the break-up of anomalous conditions in early March, 2004. Similar plots (not shown) for days prior to February 22 reveal that the "stratopause" was at or above 70 km. In the last week of that month, the mean temperature profile featured two maxima, one high up and one at a much lower altitude. Such a bifurcation is seen in the March 1 (red) profile in Figure 13. It is most likely due to contributions of different longitude sectors, some where normal conditions may have been restored and others where anomalous patterns persisted into March. In the following days, one can see the mean stratopause reform, and descend to lower altitudes—where it remains through the end of the yaw cycle. The large error bars, exceeding 20 K for much of the altitude range, imply great variability around the globe, even within the very narrow latitude range selected.

If one looks at lower latitudes (e.g., 66-69°N), one finds evidence, throughout much of the yaw cycle, of combined contributions from normal and anomalous regions. This is seen in both the zonal mean temperature profiles and their variance.

Figure 14 explicitly demonstrates, using event-by-event layer characteristics rather than mean values, two things that we discussed previously. The plots give the longitude-dependence of layer altitude, temperature, and peak VER for events in a 6-degree high-latitude bin near the end of January, 2004. They clearly show the anticorrelation of altitude, on the one hand, and temperature and VER, on the other. They also, quite obviously, illustrate the zonal asymmetry that we have mentioned.

8

One can see that the layer altitude for OH-B varies from ~77 km to ~87 km in this latitude bin, a remarkably large range that is well outside the spread of the measurements at any particular location. This explains the large variance of zonal-mean altitude for high latitudes that is shown in Figure 4f. The temperature spread of more than ~80 K is not simply an altitude effect, although one does expect higher altitudes in this region to be colder. Meanwhile, the peak VER has a range exceeding a factor of three.

The period that we chose for displaying this longitude-dependence is one for which the region with anomalous conditions is far off-center with respect to the pole, with a diminished total area (c.f., Figure 11a). This produces maximum ranges for all the layer parameters, ranges that would be considerably less (at least, for this high latitude bin) if the anomalous region were larger and more nearly centered at the pole, as in February.

It follows that although the zonal-mean plots shown earlier reveal very low altitudes and high temperatures, they actually understate the extremes of these quantities in most cases by averaging over longitude.

While reconsidering the zonal-mean layer altitude and temperature, it is worthwhile to remark again that in Figures 4 and 5 the global data that are presented there were accumulated throughout complete yaw cycles. For observations at times near local midnight, data from both mid-January and mid-March were used. However, we have now seen that anomalous conditions had disappeared well before the middle of March in both 2004 and 2006. For 2004, this means that, for these LTs, the averages combine data from normal and unusual regimes. For 2006, the mid-January dates preceded any anomalous conditions. We believe that these facts account for the appearance, in these figures, that low altitudes and large VERs do not extend as far south near midnight as at other local times for these years. In fact, the layer characteristics probably do not vary very much throughout any given day, at least not at such high latitudes where tidal influences are small. For these latitudes, variation with LT in these figures is mostly an artifact resulting from the extended duration of data-collection and slow precession of the satellite orbit.

One might ask why, for 2006 when both beginning and end of the yaw cycle observed normal conditions, there is any hint whatsoever of anomalous conditions near local midnight—as there is at the very highest latitudes in Figures 4d and 5d. The explanation is that at the "turnaround" latitudes above 80°N, where the instrument's viewing track shifts from more northerly to more southerly, observations on any orbit are smeared over a much greater range of LTs than they are at latitudes just a little bit further south. Accordingly, the northernmost LT bins include data from a much larger range of dates than other LT bins. For the highest latitudes, therefore, many observations at local midnight are from dates well into the anomalous period, two or more weeks into the yaw cycle.

2.5. Review of Other Observations

A number of papers have been published describing unusual conditions in the middle atmosphere in boreal winter 2003-2004 and/or 2005-2006. None of these discusses the OH layer and its odd characteristics, but many of the observations documented are certainly related to the behavior with which we are dealing.

Using meteorological records, Manney et al. [2005] studied trends in stratospheric vortex formation through 26 winters, highlighting extremely unusual temperatures and

winds early in what they refer to as the "remarkable" year of 2004. The observations cited extend only to ~50 km, but they document vortex breakup and re-formation at different times, as well as variations between lower and higher altitudes. The authors note that, from January on, upper stratospheric (2 hPa) temperatures were the lowest on record and the middle stratosphere was also cold. Meanwhile, the lower stratosphere (50 hPa) had record warmth and little potential for PSCs and ozone loss—hence the reference to "warm" winters in the paper's title. Their results are consistent with what we described in Section 2.3.1.

Ground-based measurements of OH rotational temperature at Resolute Bay (75°N) during the winters of 2003-2004 and 2004-2005 provided another confirmation of an anomalously warm mesosphere in the former year [*I. Azeem, private communication*].

Several satellite instruments observed enormously elevated odd nitrogen in the middle atmosphere in winter 2003-2004, and well into the spring. Such measurements are pursued because of the catalytic role of NOx in the destruction of stratospheric ozone, and because it serves as a tracer for downward transport in the polar night. The instruments included HALOE [*Natarajan et al., 2004*], ACE [*Rinsland et al., 2005*] and GOMOS [*Seppälä et al., 2004*]. The initial interpretation by these authors was that enhanced stratospheric NOx (NO plus NO_2) was a residual effect of excess NO produced at high altitudes during the intense Halloween storms of October 2003, followed by normal winter downward transport. Reviewing these and other measurements, Randall et al [*2005*] then noted the existence of the exceptionally strong polar vortex that formed in January 2004, following a major warming the previous month (both described by Manney et al. [*2005*]). They raised the possibility that greatly enhanced downwelling in the polar night together with ambient NO production could provide an alternative to the original explanation, but did not specify their preference.

Subsequently, Clilverd et al. [*2006*] studied VLF transmission through the polar vortex, which is affected by NO ionized by Ly α (from the geocorona or the Sun). They showed that storm effects had dissipated in the mesosphere by the middle of December, 2003, but that NOx increased abruptly once again around January 13, 2004—approximately a month before the first observations of enhancements in the stratosphere, and a time at which no extraordinary particle precipitation was occurring. They concluded that normal auroral production of NO in winter and strongly enhanced downward transport—rather than extraordinary production in October followed by normal downwelling—was responsible for elevated NOx in the mesosphere and (by implication) in the stratosphere as well. The VLF signal returned to normal about 37 days later, on February 19.

This is significant for our purposes because of enhanced downward transport, which affects the OH layer.

In winter 2005-2006, there was virtually no energetic particle precipitation of the kind that had occurred two years earlier. However, once again, greatly-elevated NOx was observed [*Randall et al., 2006*]. Stratospheric densities from mid-February to mid-March were higher than any on record, other than in 2004, and the stratospheric vortex was very strong. The authors came to the same conclusion as Clilverd et al. [*2006*], that very greatly-strengthened downward transport produced the anomalous result.

Meanwhile, Hauchecorne et al. [*2007*] reviewed GOMOS results for 2004 and offered a detailed explanation of the strengthened transport. They tracked much-enhanced NO_2 descending from the upper mesosphere to an altitude of ~45 km, starting between January 15 and 20 and ending in early March. They were able to identify descent rates between 0.6 and 0.2 km/day in the zonal-mean profiles, and depleted ozone at the altitudes and times where NO_2 peaked. The higher descent rate is large compared to estimates of ambient rates, which are typically a few km/month [*Randall et al., 2005*]. Their explication of the meteorology, which is qualitative, begins with the December major warming and a subsequent reversal of zonal wind in the middle stratosphere, which inhibits passage of gravity waves to higher altitudes. This removes a heat source that normally balances IR cooling in the stratopause region, which becomes anomalously cold and leads to a strong vortex re-forming there (Figure 7a) and in the lower mesosphere. Thereafter, breaking of waves at high altitudes greatly strengthens winds in the poleward direction which, in the end, induces strong downward motion, enhancing the effect of the normal summer-pole to winter-pole mesospheric meridional circulation.

Siskind et al. [*2007*] offered much the same explanation, quantitatively reinforced by model predictions. An NRL weather model, extended to the lower thermosphere with relevant chemistry, non-LTE cooling, and other additions, was initialized with meteorological winds and temperatures (blended with climatology at higher altitudes) on January 31 in both 2005 and 2006. Various parameterizations of gravity-wave forcing were used. Runs of 14 days were conducted, to see if the anomalous temperature structure from SABER and observed enhancements of NOx could be successfully simulated for mid-February.

None of the runs reproduced observed conditions exactly, but the high-latitude stratopause was displaced to ~75-80 km in 2006 (c.f. Figure 6). Its temperature was too low by ~15-20 K, which could have been due to the absence of chemical heating [*Mlynczak and Solomon, 1993*] in the model [*Siskind et al., 2007*]. Results were good for 2005, and the rate of descent of mesospheric air was much greater in 2006 than in 2005, in agreement with inferences drawn from the observations of odd-nitrogen. The authors concluded that the weak stratospheric zonal winds were responsible for suppressing gravity-wave propagation and, ultimately, producing the anomalous behavior of 2006.

2.6. Discussion

The patterns in the OH emissions that we have described seem to be consistent with the conclusions drawn from the modeling and other observations of the stratosphere in 2004 and 2006. In fact, it appears that enhanced downward transport is responsible for the low, bright OH layers in those years.

It is well established, as well as fairly obvious, that downward transport in the mesopause region brings higher concentrations of atomic oxygen into the upper mesosphere, whereas upward motion has the effect of depleting it. Atomic oxygen is directly or indirectly responsible for several layered emissions in the region, including that of OH (for which its role involves establishing the secondary ozone maximum). At most times and places, tidal effects are the predominant cause of vertical motion at these altitudes, and their effects can thus be seen in the various emissions [e.g., *Yee et al., 1997; Ward, 1999*].

Tidal influence on OH emissions can be clearly seen in Figures 3 and 5 if one focuses on equatorial regions where the strong diurnal tide is the predominant component. In almost every season, the layer is bright in the pre-midnight hours, when the flow is downward, but in the early morning, net motion is upward and the opposite is true [*Hays et al., 2003*]. At midlatitudes, brightening tends to occur shortly before local dawn, in accord with downward transport effected by the predominant semidiurnal tide [*Hays et al, 2003*]. The local times at which the motion is greatest varies with the emission altitude according to the phase of the upward-propagating tides [*Ward, 1999*], so these results would be different for the higher emissions of, for example, the O_2 Atmospheric Band.

For the high-latitude regions that are at the center of our study, such influences are relatively weak. Neither the diurnal nor semidiurnal tide is strong there, because of the nature of the waves they comprise and because some of the primary forcing mechanisms —absorption of solar radiation and latent heat release in the troposphere—are small. Therefore, little variation in brightness with local time is seen in our figures near the poles.

The downward transport at issue for our purposes, however, is induced by an entirely different mechanism. One expects no local-time dependence in this, but its effects on the airglow ought to be similar in most other respects. Assuming that the interpretation of various authors cited earlier [e.g., *Hauchecorne et al., 2007; Siskind et al., 2007*] is correct, very strong downwelling is occurring during the anomalous periods we have identified. The result of this should be exactly the brightening we observe.

We note that Ward [*1999*] showed that, in the tidal regime, the effect of downward transport (which is mainly increased O) trumps the simultaneous effects (which are opposite in sign) of temperature and density changes on the emission intensity. It is reasonable to assume that the same holds true for downwelling in polar winter.

We did not remark upon it earlier, but GOMOS was able to track the ozone maximum in the upper mesosphere during the period January 1-18, 2004 [*Hauchecorne et al., 2007*]. After about the 10th, there was a clear lowering of the altitude at which this was seen, from ~80 km to ~ 75 km. These authors' interpretation was of rapid descent of air rich in Ox. In consideration of the mechanism for forming hydroxyl, it is clear that such occurrences would result in a lower-than-normal OH layer. The timing coincides quite closely with the date (the 13th, within a day) determined by Clilverd et al. [*2006*] for the onset of enhanced NO^+ in the mesosphere that year.

All the observations we have cited appear to be consistent with each other, and they all point to enhanced downward transport of atomic oxygen from the thermosphere being responsible for the very low and bright OH layer. Considering that anomalies in the mesosphere and lower thermosphere are likely the result of perturbed circulation in the stratosphere that suppresses gravity wave propagation from the troposphere, these observations provide an interesting example of the interconnectedness of the various atmospheric regions. Given that the emissions can be observed quite easily, they also offer the possibility that a very low, bright OH layer could serve as a proxy for perturbed meteorological conditions in polar winter.

2.7. Summary and Conclusions

In this report, we have presented evidence of previously unreported characteristics of the otherwise familiar hydroxyl emissions in the upper mesosphere. In two of the six years to date that the TIMED satellite has been aloft, the SABER instrument observed unusually bright emissions from unusually low altitudes, often below 80 km, in the high-latitude boreal winter. Using volume emission rates derived from the observed limb radiance, we show that that these anomalous conditions existed from at least mid-January into early March of 2004, and for approximately the month of February 2006. Although confined to locations polewards of ~60°N, the regions where they appeared were neither zonally symmetric nor static. Variations occurred on a time scale of many days. No such behavior was observed in 2002, 2003, 2005, or 2007, nor in any southern polar winter.

At the same time, SABER retrieved temperature also had very unusual characteristics. A distortion of the normal thermal structure of the middle atmosphere occurred during those winters, making the ~40-60 km altitude region very cold and displacing the strato-pause to ~70-80 km. Temperatures as high as ~280 K were recorded there on some days, and even zonal-mean temperatures exceeded 260 K with regularity.

We have shown that the anomalous temperature and OH layer characteristics are tight-ly correlated. At the times and places where the layers are low, they are also bright, and the temperature at the layer altitude is unusually warm. Conversely, where the layers are close to the nominal altitude of 87 km, they are one-half to one-third as bright and the temperature is much lower.

A number of papers published in the past two years describe anomalous conditions in 2004 and 2006, although none discuss the OH layer characteristics. To the extent that comparisons are possible, their results are consistent with SABER retrieved temperature. Many of them focus on odd nitrogen in the middle atmosphere, which was unusually high. The consensus that emerges was that the elevated NOx, which serves as a tracer in polar night, was the result of greatly elevated downwelling in the vortex. A modeling exercise [*Siskind et al., 2007*] supported this conclusion. It also provided a meteorologi-cal explanation, with unusual stratospheric winds ultimately being responsible because of their effect in suppressing normal gravity-wave activity.

Enhanced downward transport is completely consistent with the observations of anom-alous OH layer characteristics, and provides a likely explanation for them. In this scen-ario, strong downwelling brings more atomic oxygen from above the mesopause down to altitudes where ozone forms, resulting in greater concentrations of ozone and more rapid formation of excited OH. If a combination of unusual tropospheric and stratospheric con-ditions are indeed responsible for the downwelling, the implication is that easily observed OH emissions could serve as a proxy for such conditions, as well as for associated anom-alous temperatures in the mesosphere.
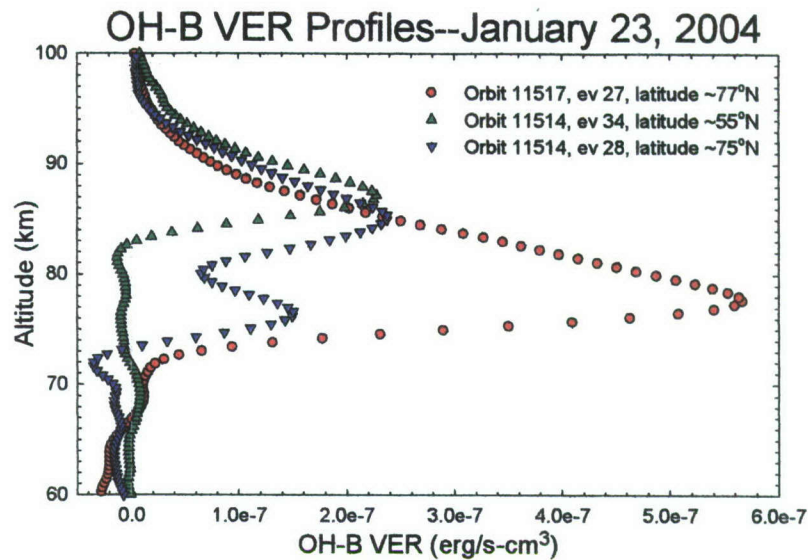
OH-B VER Profiles--January 23, 2004

Figure 1. OH-B VER profiles, including one low-altitude peak (red), one "normal" peak (green), and one double peak (blue). See text.
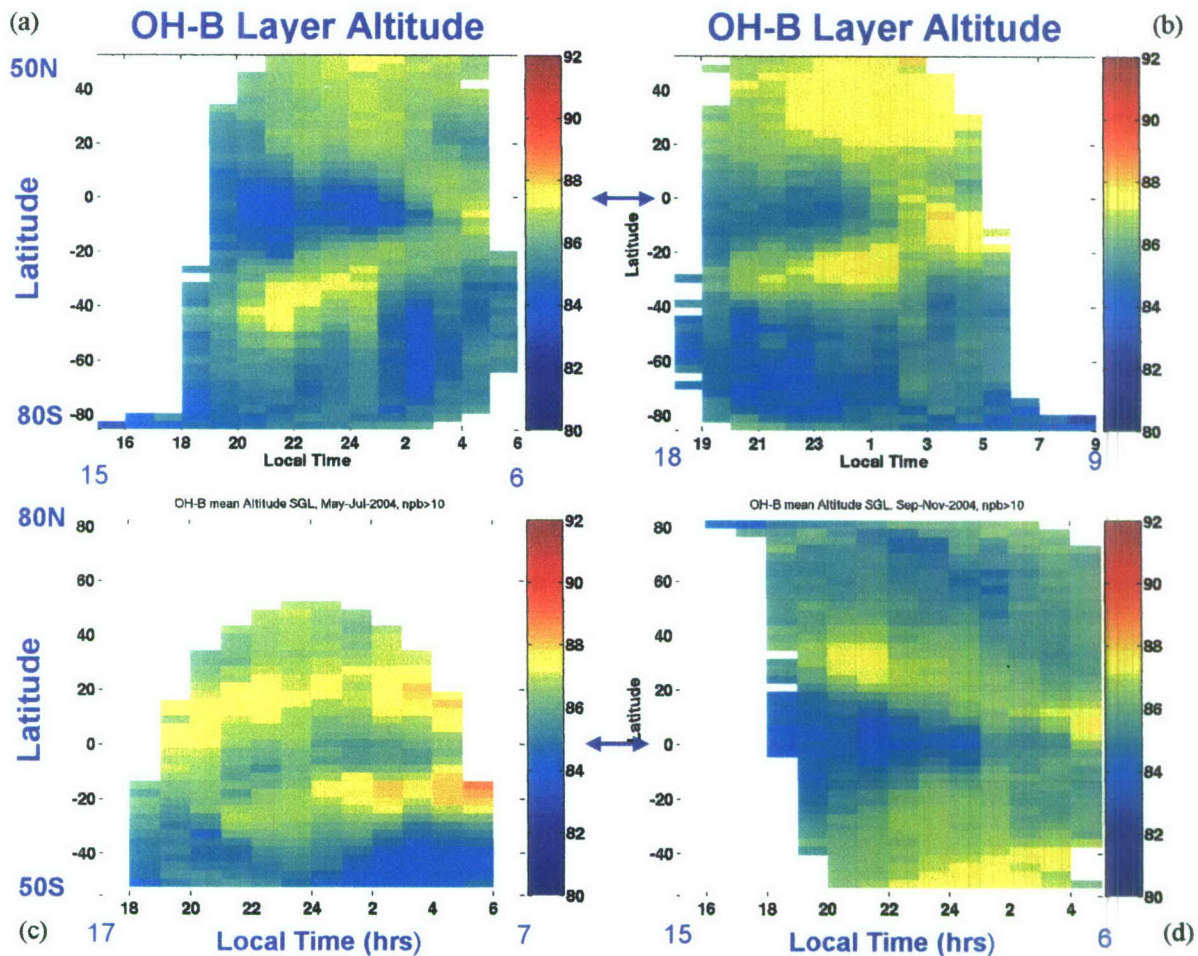
OH-B Layer Altitude

Figure 2. OH-B layer altitude (km) for four yaw cycles in 2004. (a) March 18-May 21; (b) July 15-Sept. 21; (c) May 21-July 15; (d) Sept. 21-Nov. 20. The blue double arrows indicate the equator. The north-viewing May-July cycle appears truncated due to lack of nighttime conditions in the Arctic summer.
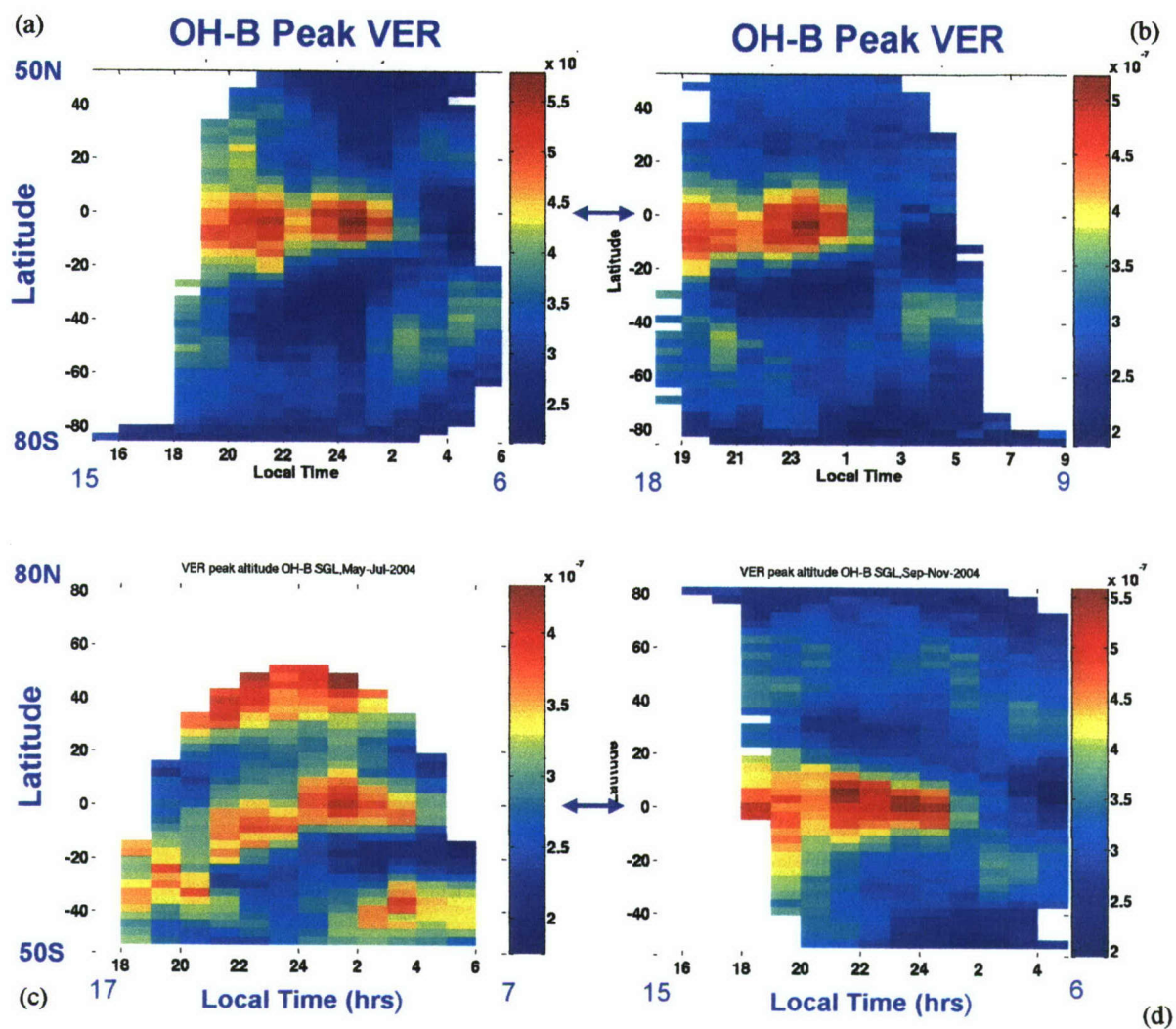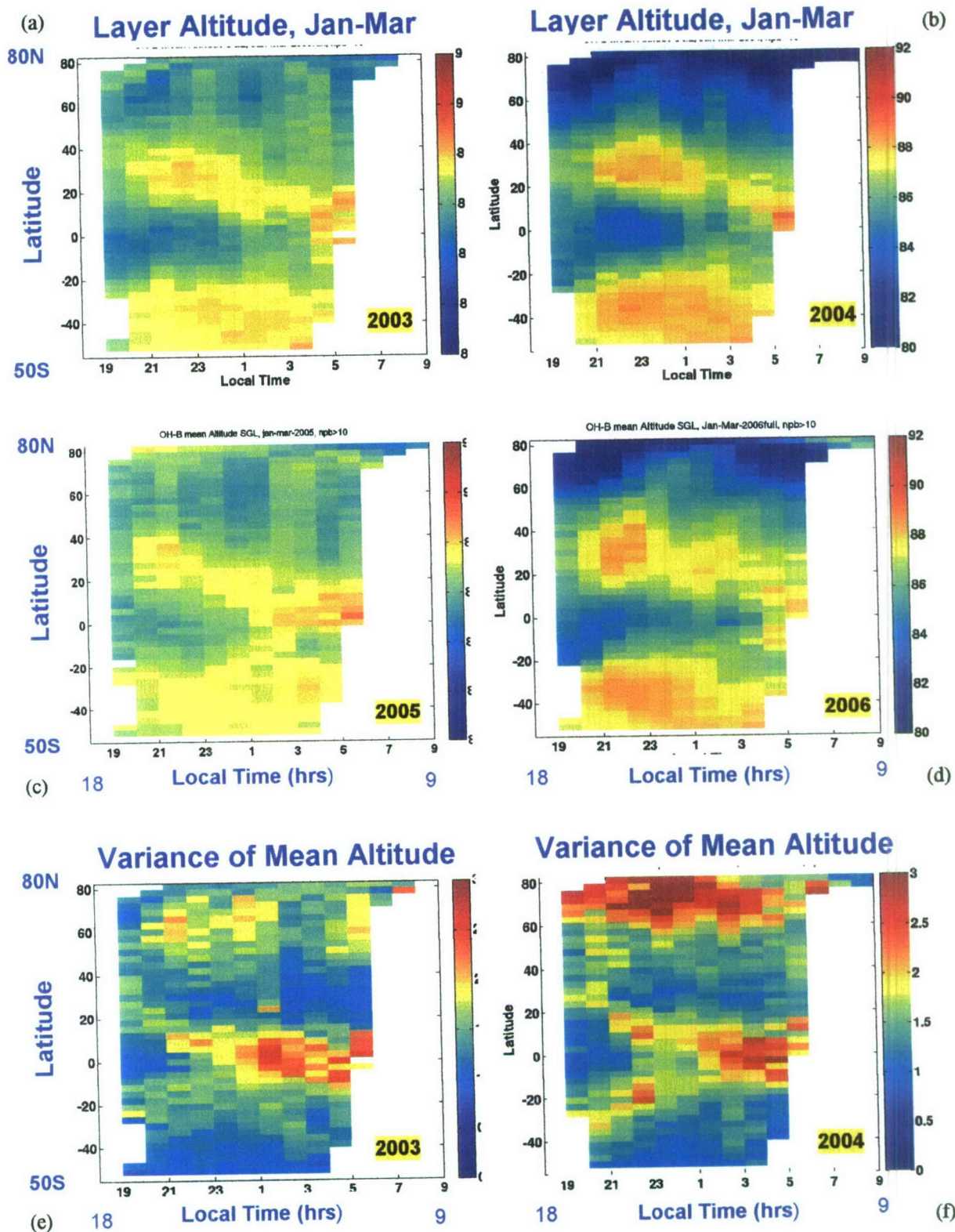
Figure 3. As in Figure 2, but the quantity plotted is the mean OH-B peak volume emission rate (VER, in units of erg/s-cm^3) for four yaw cycles in 2004. (a) March 18-May 21; (b) July 15-Sept. 21; (c) May 21-July 15; (d) Sept. 21-Nov. 20.

Figure 4. Latitude/local time plots of layer altitude and altitude variance (OH-B) for January-March yaw cycles. (a) altitude, 2003; (b) altitude, 2004; (c) altitude, 2005; (d) altitude, 2006; (e) variance, 2003; (f) variance, 2004. The anomalous regions are found at the northernmost latitudes in 2004 and 2006.
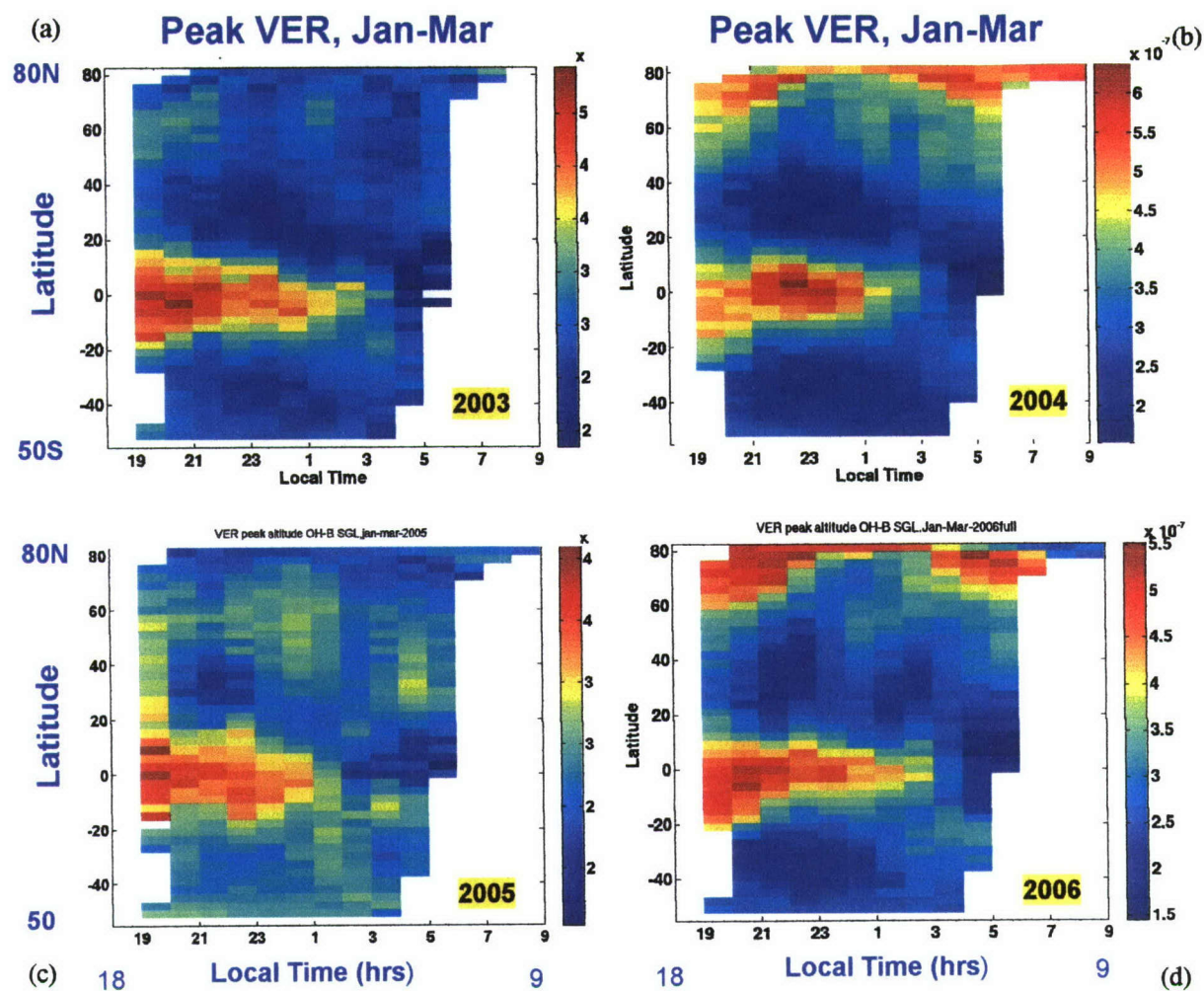
Figure 5. Latitude/local time plots of layer brightness (OH-B) for January-March yaw cycles. (a) 2003; (b) 2004; (c) 2005; (d) 2006.
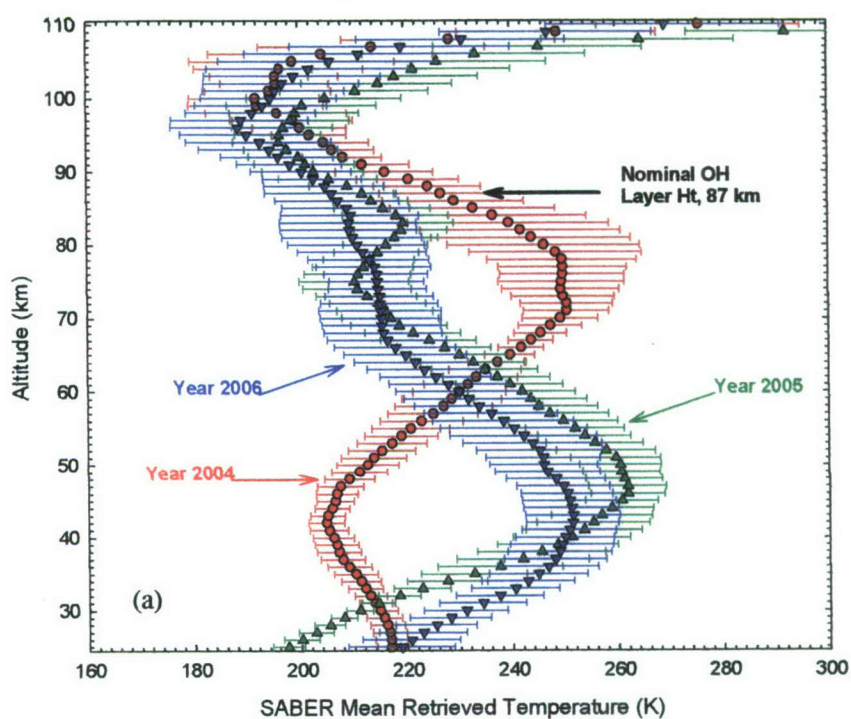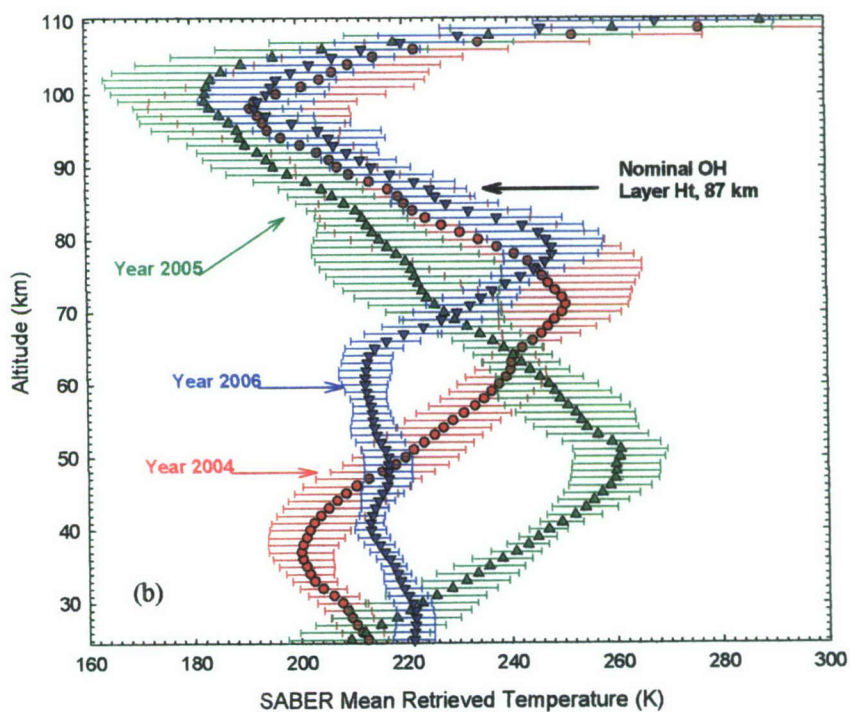
Figure 6. Comparison of zonal-mean retrieved temperature in the latitude range 75-78°N, for two days in boreal winters 2004 (red), 2005 (green), and 2006 (blue). (a) January 19; (b) February 4. Error bars are 1-sigma.
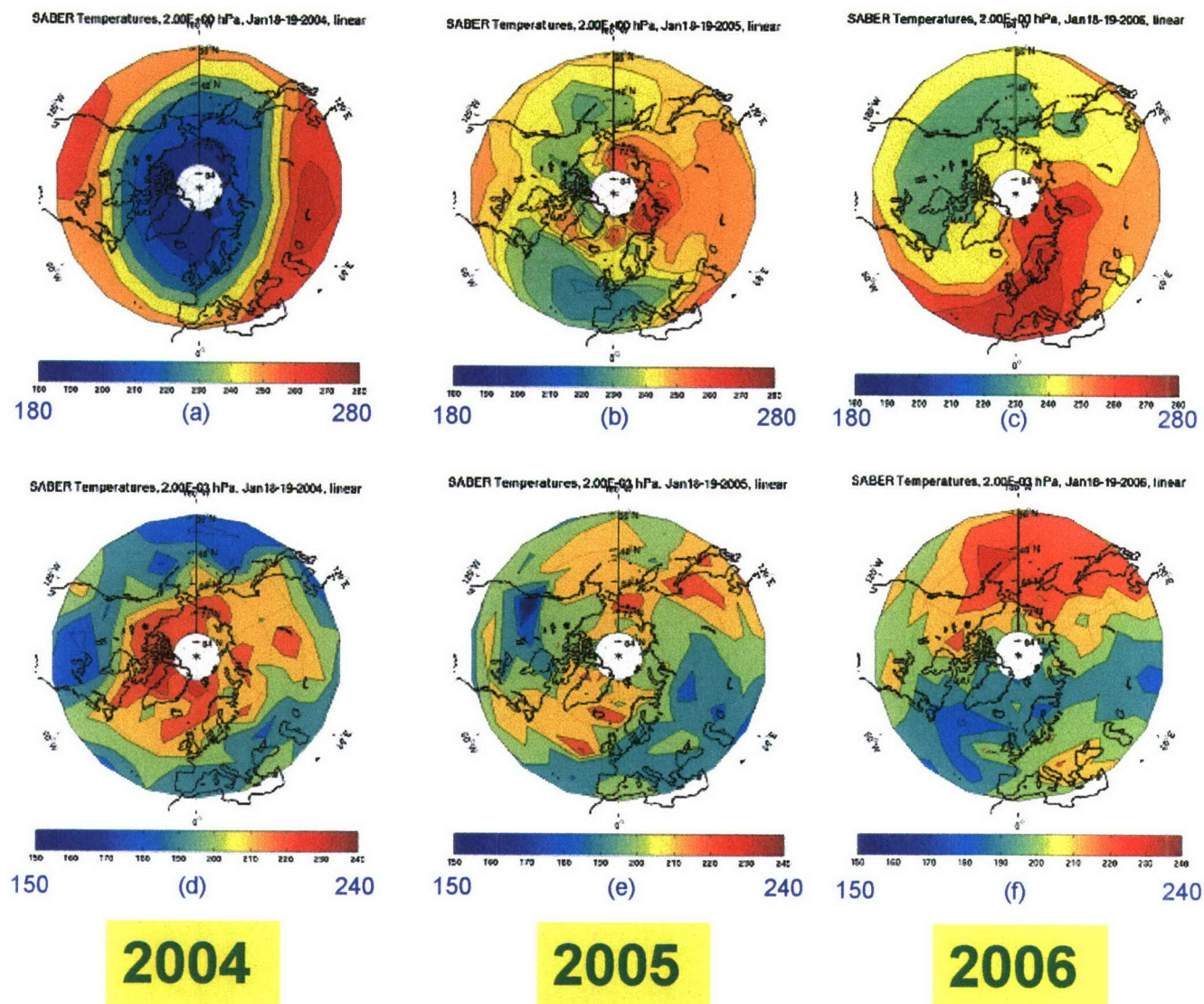
2004   **2005**   **2006**

Figure 7. Interannual comparison of stratospheric (top) and mesospheric (bottom) temperature for January 18-19. SABER retrieved temperature in the northern hemisphere, down to 30°N, is plotted at 2 hPa for those days in (a) for 2004; (b) for 2005; and (c) for 2006. It is plotted at 0.002 hPa in (d) for 2004; (e) for 2005; (f) for 2006. The temperature color scale ranges from 180 to 280 K for the stratosphere maps, and 150 to 240 K for the mesosphere.
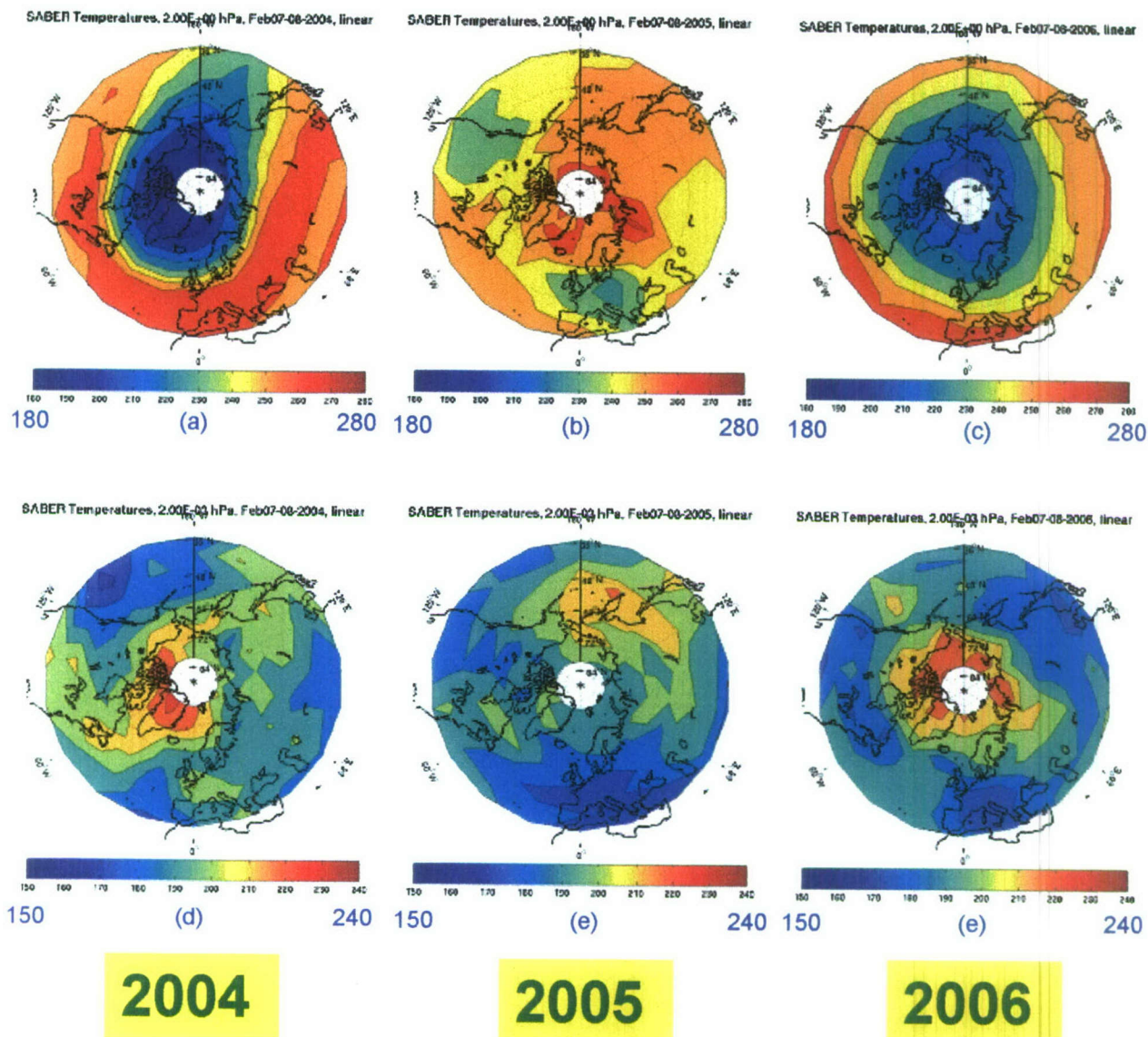
2004   **2005**   **2006**

Figure 8. Interannual comparison of stratospheric (top) and mesospheric (bottom) temperature for Febuary 7-8. SABER re-trieved temperature in the northern hemisphere, down to 30°N, is plotted at 2 hPa for those days in (a) for 2004; (b) for 2005; and (c) for 2006. It is plotted at 0.002 hPa in (d) for 2004; (e) for 2005; (f) for 2006. The temperature color scale ranges from 180 to 280 K for the stratosphere maps, and 150 to 240 K for the mesosphere.
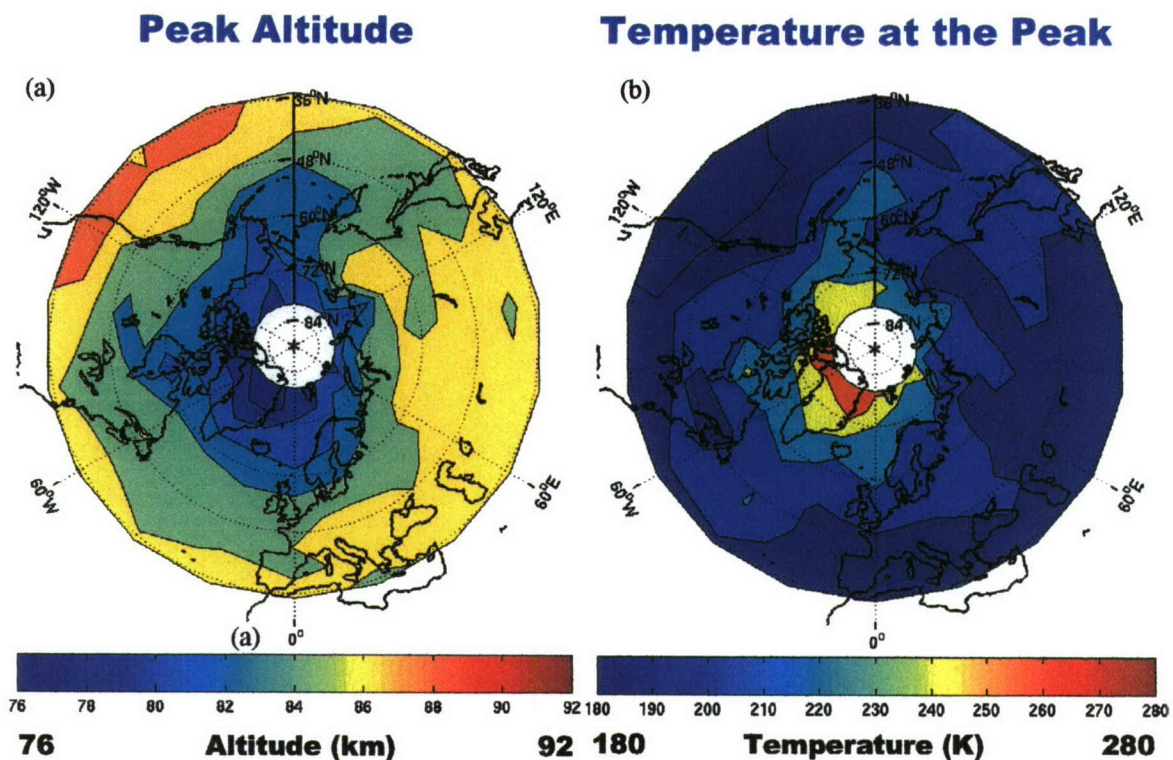
Peak Altitude

(a)

Temperature at the Peak

(b)

76   Altitude (km)   92   180   Temperature (K)   280

Figure 9. Correlation of (a) OH layer altitude and (b) SABER retrieved temperature at the layer altitude, Feb.7-8, 2004
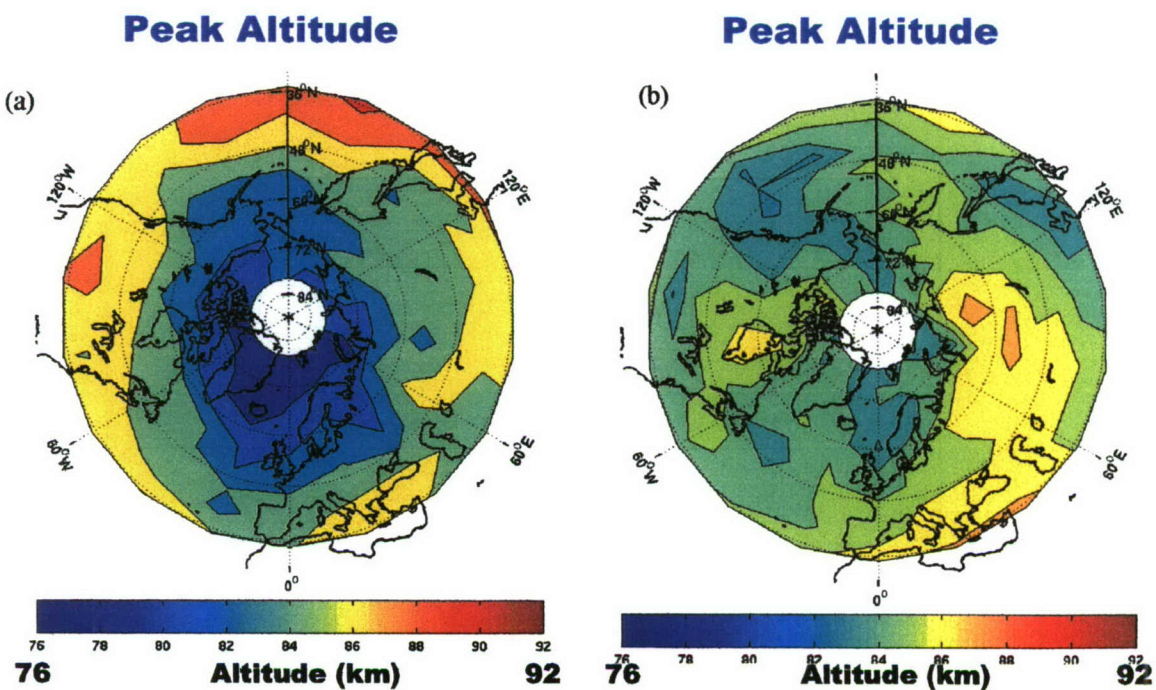
Peak Altitude

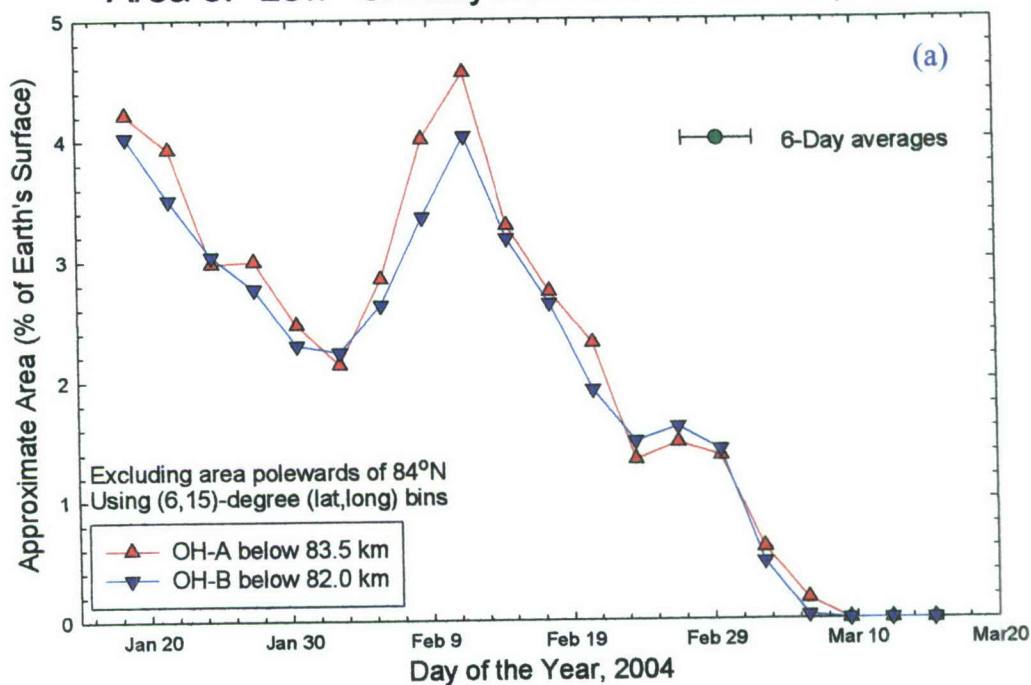(a)

Peak Altitude

(b)

76   Altitude (km)   92   76   Altitude (km)   92

Figure 10. OH layer altitude on January 18-19 in two different years. (a) 2004; (b) 2005
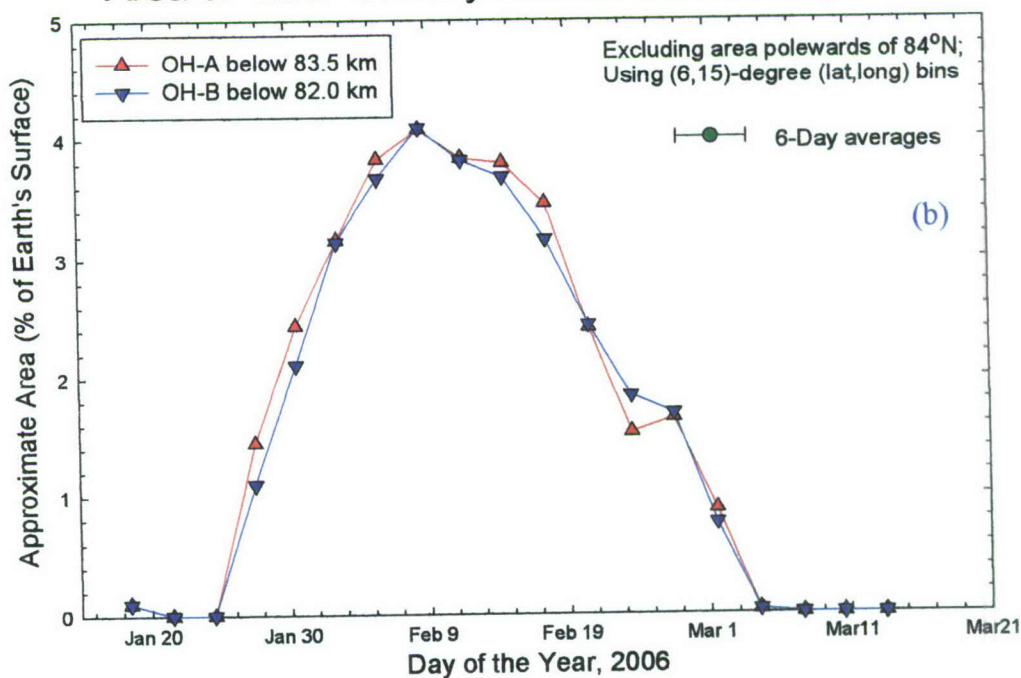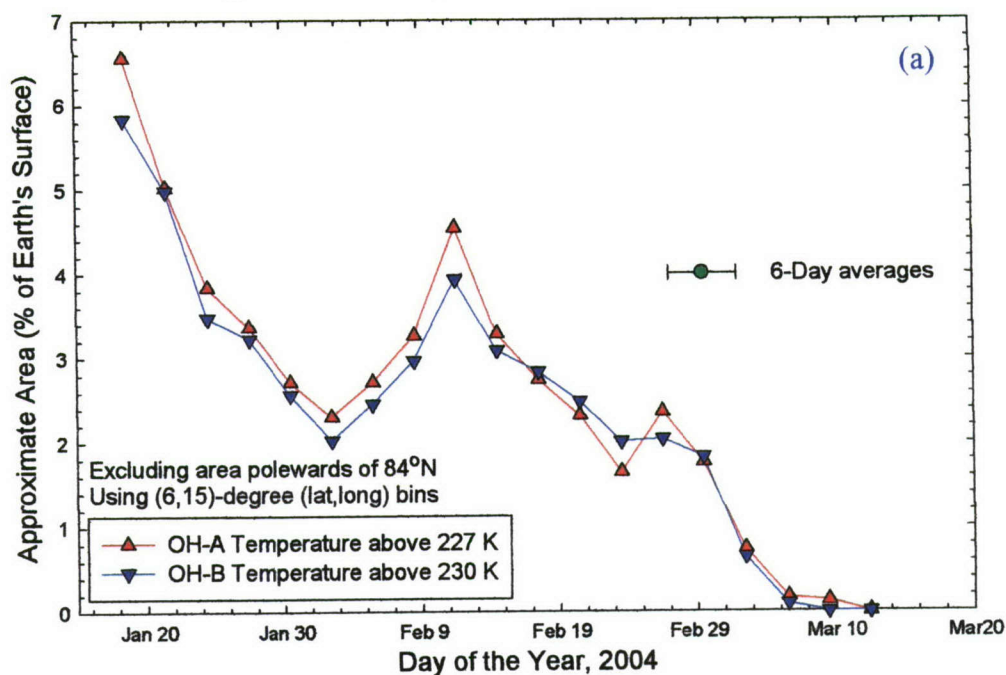
22

Figure 11. Percentage of Earth's surface characterized by low-altitude OH layers from mid-January to mid-March. (a) 2004; (b) 2006

Area of "High" OH Temperatures in Boreal Winter, 2004
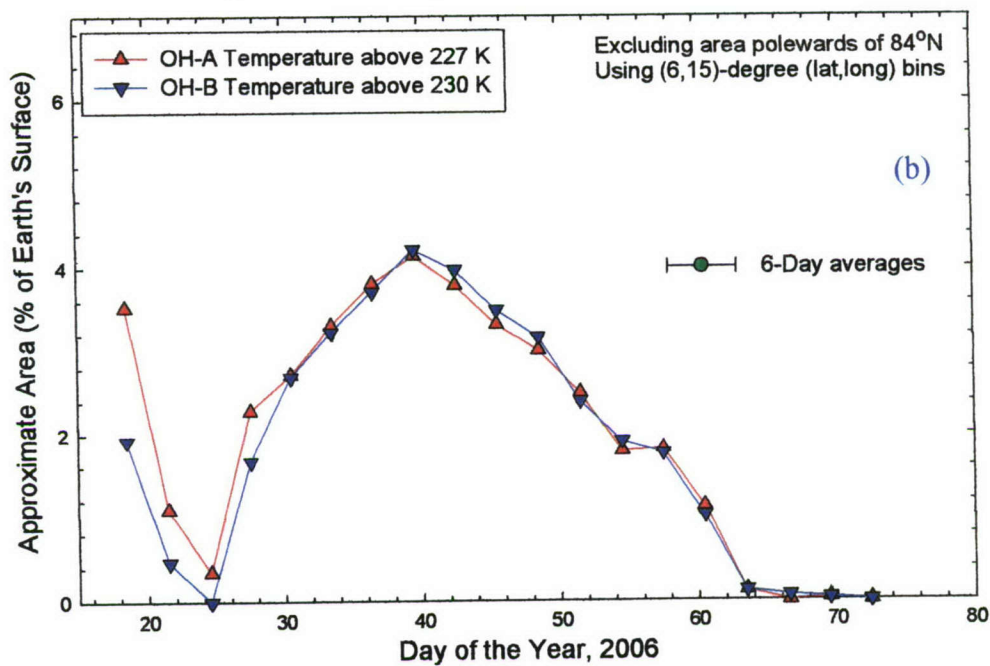

(a)

Figure 12. Percentage of Earth's surface characterized by high temperatures at the altitude of the OH layer from mid-January to mid-March. (a) 2004; (b) 2006
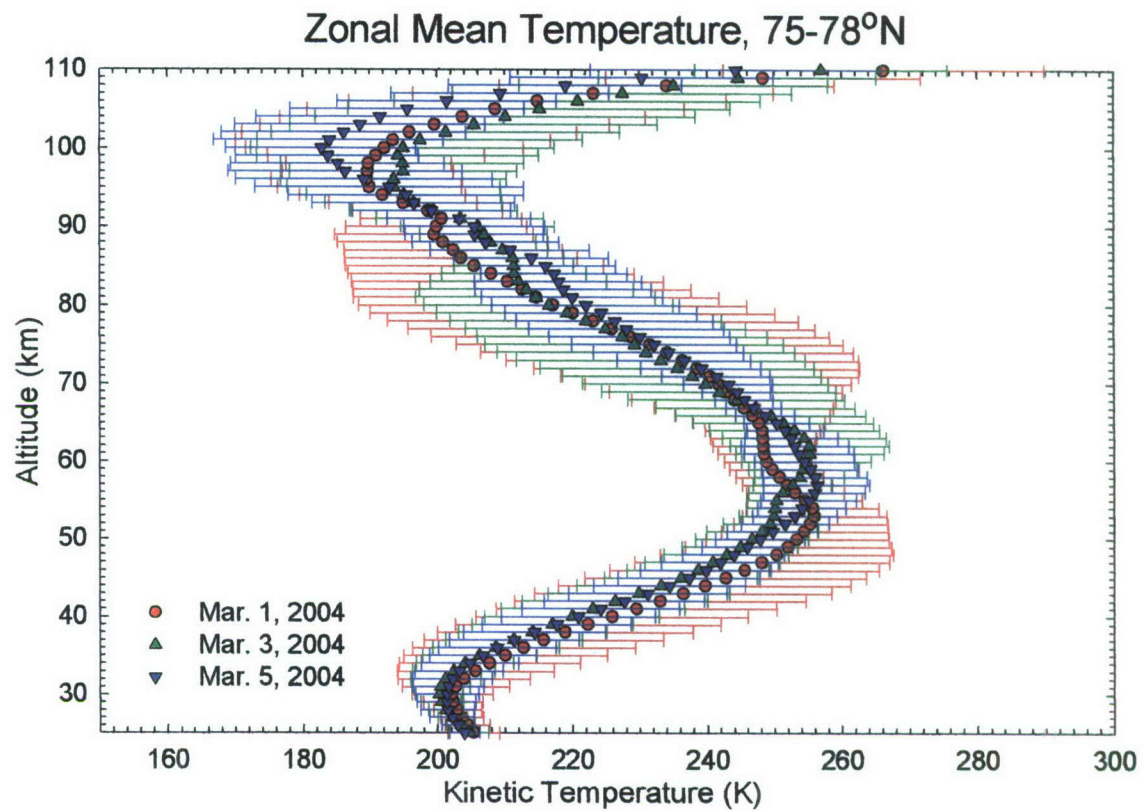
Figure 13. Zonal-mean retrieved temperature in the latitude range 75-78°N, for three days in early March 2004, near the end of the period of anomalous conditions. Error bars are 1-sigma.
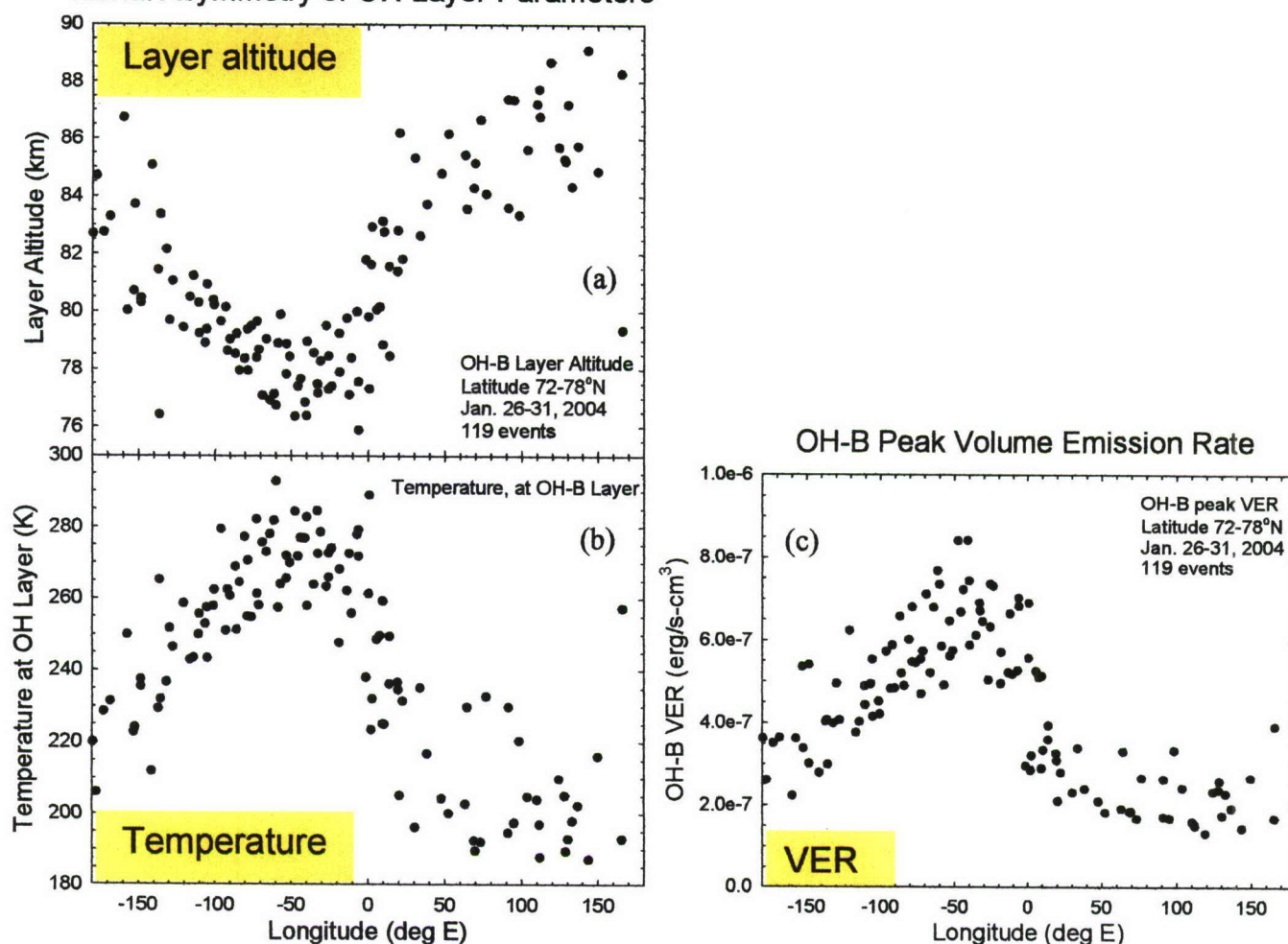
Figure 14. Longitude-dependence of OH layer properties, using all SABER nighttime single-peak events in a 6-degree latitude bin (72-78°N) for a 6-day period near the end of January, 2004. (a) Layer altitude; (b) temperature at the layer altitude; (c) VER at the layer altitude.

REFERENCES

Clilverd, M.A., A. Seppälä, C.J. Rodger, P.T. Verronen, and N.R. Thompson, "Ionospheric evidence of thermosphere-to-stratosphere descent of polar NOx", *Geophys. Res. Lett.*, **33**, L19811, doi:10.1029/2006GL026727, 2006.

Hauchecorne, A., J.-L. Bertaux, F. Dalaudier, J.M. Russell III, M.G. Mlynczak, E. Kyrölä, and D. Fussen, "Large increase in NO_2 in the north polar mesosphere in January-February 2004: Evidence of a dynamical origin from GOMOS/ENVISAT and SABER/TIMED data", *Geophys. Res. Lett.*, **34**, L03810, doi:10.1029/2006GL027628, 2007.

Hays, P.B., J.F. Kafkalides, W.R. Skinner, and R.G. Roble, "A global view of the molecular oxygen nightglow", *J. Geophys. Res.*, **108**(D20), 4646, doi:10.1029/2003JD 003400, 2003.

Manney, G.L., K. Krüger, J.L. Sabutis, S.A. Sena, and S. Pawson, "The remarkable 2003-2004 winter and other recent warm winters in the Arctic stratosphere since the late 1990s", *J. Geophys. Res.*, **110**, D04107, doi:10.1029/2004JD005367, 2005.

Melo, S.M.L., R.P. Lowe, and J.P. Russell, "Double-peaked hydroxyl airglow profiles observed from WINDII/UARS", *J. Geophys. Res.*, **105**, 12397-12403, 2000.

Mertens, C.J., M.G. Mlynczak, M. Lopez-Puertas, P.P Wintersteiner, R.H. Picard, J.R. Winick, L.L. Gordley, and J.M. Russell III, "Retrieval of mesospheric and lower thermospheric kinetic temperature from measurements of CO_2 15 μm Earth limb emission under non-LTE conditions", *Geophys. Res. Lett.*, **28**, 1391-1394, 2001.

Mertens, C.J., M.G. Mlynczak, M. Lopez-Puertas, P.P Wintersteiner, R.H. Picard, J.R. Winick, L.L. Gordley, and J.M. Russell III, "Retrieval of kinetic temperature and carbon dioxide abundance from non-local thermodynamic equilibrium limb emission measurements made by the SABER experiment on the TIMED satellite", *Proc SPIE*, **4882**, 162-171, 2002.

Mertens, C.J., F.J. Schmidlin, R.A. Goldberg, E.E. Remsberg, W.D. Pesnell, J.M. Russell III, M.G. Mlynczak, M. Lopez-Puertas, P.P. Wintersteiner, R.H. Picard, J.R. Winick, and L.L. Gordley, "SABER observations of mesospheric temperatures and comparisons with falling sphere measurements taken during the 2002 summer MaCWAVE campaign", *Geophys. Res. Lett.*, **31**, L03105, doi:10.1029/2003GL018605, 2004.

Mlynczak, M. and S. Solomon, "A detailed evaluation of the heating efficiency in the middle atmosphere", *J. Geophys. Res.*, **98**, 10517-10541, 1993.

Mlynczak, M., F.-J. Martin-Torres, G. Crowley, D.P. Kratz, B. Funke, G. Lu, M. Lopez-Puertas, J.M. Russell III, J. Kozyra, C. Mertens, R. Sharma, L. Gordley, R. Picard, J. Winick, and L. Paxton, "Energy transport in the thermosphere during the solar storms of April 2002", *J. Geophys. Res.*, **110**, A12S25, doi:10.1029/2005JA011141, 2005.

Natarajan, M., E.E. Remsberg, L.E. Deaver, and J.M. Russell III, "Anomalously high levels of NOx in the polar upper stratosphere during April, 2004: Photochemical consistency of HALOE observations", *Geophys. Res. Lett.*, **31**, L15113, doi:10.1029/2004 GL020566, 2004.

Randall, C.E., V.L. Harvey, G.L. Manney, Y. Orsolini, M. Codrescu, C. Sioris, S. Bro-hede, C.S. Haley, L.L. Gordley, J.M. Zawodny, and J.M. Russell III, "Stratospheric effects of energetic particle precipitation in 2003-2004", *Geophys. Res. Lett.*, **32**, L05802, doi:10.1029/2004GL022003, 2005.

Randall, C.E., V.L. Harvey, C.S. Singleton, P.F. Bernath, C.D. Boone, and J.U. Kozyra, "Enhanced NO_x in 2006 linked to strong upper stratospheric Arctic vortex", *Geophys. Res. Lett.*, **33**, L18811, doi:10.1029/2006GL027160, 2006.

Rinsland, C.P., C. Boone, R. Nassar, K. Walker, P. Bernath, J.C. McConnell, and L. Chou, "Atmospheric Chemistry Experiment (ACE) Arctic stratospheric measurements of NOx during February and March 2004: Impact of intense solar flares", *Geophys. Res. Lett.*, **32**, L16S05, doi:10.1029/2005GL022425, 2005.

Russell, J.M. III, M.G. Mlynczak, L.L Gordley, J. Tansock, and R. Esplin, "An overview of the SABER experiment and preliminary calibration results", *Proc. SPIE*, **3756**, 277-288, 1999.

Seppälä, A., P.T. Verronen, E. Kyrölä,, S. Hassinen, L. Backman, A. Hauchcorne, J.L. Bertaux, and D. Fussen, "Solar proton events of October-November 2003: Ozone depletion in the Northern Hemishere polar winter as seen by GOMOS/Envisat", *Geophys. Res. Lett.*, **31**, L19107, doi:10.1029/GL021042, 2004.

Seppälä, A., P.T. Verronen, M.A. Clilverd, C.E Randall, J. Tamminen, V. Sofieva, L. Backman, and E. Kyrölä, "Arctic and Antarctic polar winter NO_x and energetic particle precipitation in 2002-2006", *Geophys. Res. Lett.*, **34**, L12810, doi:10.1029/2007GL029 733, 2007.

Siskind, D.E., L. Coy, and P. Espy, "Observations of stratospheric warmings and mesospheric coolings by the TIMED SABER instrument", Geophys. Res. Lett., 32, L09804, doi:10/10292005GL022399, 2005.

Siskind, D.E., S.D. Eckermann, L. Coy, J.P. McCormack, and C.E. Randall, "On recent interannual variability of the Arctic winter mesosphere: Implications for tracer descent", *Geophys Res. Lett.*, **34**, L09806, doi:10.1029/2007GL029293 (2007).

Ward, W.E., "A simple model of diurnal variations in the mesospheric oxygen nightglow", *Geophys. Res. Lett.*, **26**, 3565-3568, 1999.

Winick, J.R., P.P. Wintersteiner, R.H. Picard, C.J. Mertens, M.G. Mlynczak, M.E. Hagan, W.E. Ward, J.M. Russell, and L.L. Gordley, "Global occurrence statistics of mesospheric inversion layers obtained from SABER temperature profiles", *Eos Trans. AGU*, **85**(46), Fall Meet. Suppl., Paper SA34A-06, 2004.

Winick, J.R., P.P. Wintersteiner, R.H. Picard, M.J. Taylor, D. Baker, M.G. Mlynczak, J.M. Russell III, and L.L. Gordley, "Global statistics of OH layer heights and double layers from SABER limb measurements of OH Meinel emission at 1.6 and 2.0 μm", *Eos Trans. AGU*, **86**(47), Fall Meet. Suppl., Paper SA43A-1095, 2005

Winick, J.R., R.H. Picard, P.P. Wintersteiner, D. Esplin, M.J. Taylor, I. Azeem, M.G. Mlynczak, J.M. Russell III, L.L. Gordley, and G. Crowley, "Interannual variability of OH Meinel emission as determined from SABER limb measurements at 1.6 and 2.0 microns", *EOS Trans AGU*, **87**(47), Fall Meeting Supplement, SA21-0224, 2006.

Wintersteiner, P.P, and E. Cohen, "Observations and modeling of the upper mesosphere: Mesopause properties, inversion layers, and bores", Air Force Research Laboratory Technical Report, AFRL-VS-HA-TR-2005-1162, 2005.

Yee, J.-H., G. Crowley, R.G. Roble, W.R. Skinner, M.D. Burrage, and P.B. Hays, "Global simulations and observations of O(1S), O2(1Σ) and OH mesospheric nightglow emissions", *J. Geophys. Res.*, **102**(A9), 19949-19968, 1997.

Zhang, S.P., and G.G. Shepherd, "The influence of the diurnal tide on the O(^{1}S) and OH emission rates observed by WINDII on UARS", Geophys Res. Lett., 26, 529-532, 1999.

APPENDIX

This appendix describes an algorithm we devised, to eliminate events that appear to be faulty in certain respects and to distinguish between single- and multiple-peak events.

It is common to find SABER event profiles with negative retrieved VER at altitudes well below the main OH peak. This unphysical behavior is probably due to inherent difficulties in the inversion process, considering the steep gradient at these altitudes and noise in the input signal. Such features are apparent in all three events depicted in Figure 1, and we simply ignore those parts of the profiles. Occasionally, however, we identify negative regions at higher altitudes, or large negative-going spikes. The discrimination algorithm rejects all events for which the VER of OH-A or OH-B has any point below a small negative threshold, for any altitude above the main peak or above 84 km. (The threshold is -1×10^{-8} erg/s-cm^3 for OH-A and twice that for OH-B. In absolute terms, this is $\sim$5-10% of a typical peak.) We also reject events with a large negative spike anywhere, "large" being five times the threshold. For a typical yaw cycle, a few hundred (out of $\sim$45,000) nighttime events fail these tests.

Our algorithm also rejects events with main peaks having a full-width (at half maximum) of 2 km or less, and events with the VER peak above 95 km. Those cases are quite unusual.

To identify multiple peaks, it is often necessary to consider ambiguous characteristics. Many VER profiles contain a main peak with a prominent "shoulder" on it, a main peak with closely-spaced local maxima, or a main peak plus one or more small but distinct subsidiary peaks. The algorithm we wrote distinguishes among such events, in addition to identifying those with clearcut double peaks.

VER profiles with shoulders are qualitatively similar to profiles with the ordinary asymmetry, noted above in Section 2.2.1., that results from, among other things, differences in the gradients of H and O_3. Although many of these resemble unresolved double peaks that could be separated using a nonlinear fitting procedure, we regard them as single-peak events.

When a secondary maximum does appear, we accept it as such if it is at least 25% as high as the primary peak, more than 1 km above or below the intervening minimum, and more than 2 km in width. Peaks more than 15% as high are also accepted, provided that (in addition) the VER at the intervening minimum is less than 93% of that at the smaller peak. In both cases, points in the immediate vicinity of the local maximum must survive certain requirements that rule out noise-induced artifacts, and that guarantee that a low-order polynomial fit can be performed. Fits provide the best estimate of peaks' locations and sizes; they are also done for primary peaks.

As noted earlier, events for which we identify double peaks in the OH-A or OH-B VER profiles have not been used in our study. Figure 1 shows one such event.